Heterogeneous Distribution of Technetium-99m-Labeled Microspheres in Rat Lungs: Microautoradiographic Evidence and Dosimetric Consequences

Marjorie S. Robinson, Nicole C. Colas-Linhart, Françoise M. Guiraud-Vitaux, Anne M. Petiet and Bernard D. Bok
Department of Biophysics, School of Medicine, Xavier Bichat University, Paris; and Radioisotopes Department, Montfermeil Hospital, Montfermeil, France

The heterogeneity of ^{99m}Tc-labeled microspheres distribution within rat lung was visualized and quantified using a microautoradiographic "track" method (MAR). **Methods:** MAR was used to study the uptake of radioactivity by individual microspheres, thereby enabling calculation of the range of particle activity. MAR was also used to visualize in rat lung sections the intrapulmonary distribution of the microspheres within the lungs after intravenous administration. The mean doses delivered to the cells in close contact with the labeled microspheres were calculated taking only the ^{99m}Tc electron emissions into account. **Results:** All the microspheres were labeled. Nevertheless, the spectrum of visible tracks varied by a factor of 10, inducing a variable activity per microsphere from <36 Bq to 325 Bq (mean activity = 94 Bq/microsphere). No correlation existed between the radioactivity uptake and the size of microspheres. A very heterogeneous tridimensional distribution of the microspheres within the lungs were demonstrated with interparticle distances ranging from 57–4400 μm. On the other hand, only 1 of 2000 rat lung capillaries was obstructed. Using the mean activity, calculated delivered doses were found to reach approximatly 6 Gy for the closest endothelial cells and 2 Gy for epithelial cells. However, such high doses were delivered to only a few cells. **Conclusion:** The number of obstructed capillaries in human lungs is lower than in rat lungs; the distances between microspheres should be larger. Nevertheless, the individual doses absorbed by the pulmonary cells closest to the microspheres should be very important.

Key Words: microautoradiography; technetium-99m-labeled microsphere; cellular dosimetry; rat lungs

J Nucl Med 1997; 38:650–654

In nuclear medicine, most dosimetric evaluations assume that the distribution of the radiopharmaceutical within the organ of interest is uniform. Conventional methods for calculating the radiation dose delivered to an organ implicitly postulate that the dose to all cells of a given organ is the same as the integral dose. Numerous studies established that there are both heterogeneity of localization and heterogeneity of radiation emissions (*1–4*). Absorbed dose heterogeneity may be more disparate when the radioactivity is electively concentrated in particular types of cells, and the range of the electron is small. Lung imaging using intravenous injection of radiolabeled albumin particles has been available since 1968 (*5*) and has been considered to be reasonably safe (*6*). In a previous study (*7*), we showed that the dose absorbed by *radiolabeled* Kupffer cells after ^{99m}Tc-sulfur colloid injection was approximately 15,000 times the mean electron dose to the same cells as estimated using the conventional MIRD Schema (*8*). Earlier, Makrigiorgos et al. (*9*) used a computer program based on a theoretical model that accounted for the nonuniform distribution of ^{99m}Tc-labeled microspheres and macroaggregates to calculate the doses delivered to lung cells by ^{99m}Tc electrons and photons. The dose to 8% of the cell population was very high (3–7500 times the MIRD estimate). The authors concluded that a more rigorous microdosimetric evaluation would require experimental information regarding the spectrum of sizes of microspheres, the radioactivity taken up individually by these microspheres and once injected, their spatial distribution throughout the lungs.

For this purpose, in this study, we applied an appropriate experimental technique, the MAR "track" method adapted to the detection of high-energy internal conversion electrons of ^{99m}Tc (*10*). This method is able to detect the whole path of these electrons through the overlaying emulsion. Using a thicker emulsion layer and 24 hr exposure (93% of disintegrations), a gold latensification enhanced the visualization of "tracks" (defined as at least five consecutive silver grains) (*11*). MAR has been successfully applied to ^{99m}Tc-labeled leukocytes and to the uptake of ^{99m}Tc colloids by the Kupffer cells in tissue sections (*10,12*). The aim of the study was first to visualize and quantify the uptake of radioactivity by individual particles, and second, to image their spatial distribution within the rat lungs. A simple model is proposed to calculate the corresponding radiation doses delivered to the pulmonary cells in contact with the microspheres.

MATERIALS AND METHODS

In Vitro Studies

The ^{99m}Tc-labeled microspheres (Sferotec-S, Sorin, Italy) were prepared according to the manufacturer's instructions. Sterile sodium pertechnetate (5 ml), with an activity of 0.6 GBq (16 mCi), was introduced into the vial containing the microspheres (about 4.10^6/vial). The radiochemical purity was verified after labeling. The labeling efficiency was about 96% 5 min after the addition of pertechnetate ($^{99m}TcO_4^-$) and remained unchanged for 72 hr.

The size distribution of the microspheres after reconstitution with 0.9% NaCl or $^{99m}TcO_4^-$ was assessed. The wet microspheres were deposited under a Malassez cell. Their numbers and individual diameters were determined under an optical microscope using a micrometric scale.

The MAR track technique was performed as described previously (*10,12*). Briefly, a nuclear emulsion (K5 Ilford) was poured onto gelatin-coated slides to obtain a coating 25 μm thick. After 24 hr of exposure, a gold latensification is necessary to transform the sublatent into a latent image. Then, the preparation is developed and fixed. MAR was first used immediately after labeling microspheres to evaluate the percentage of labeled microspheres. However, the amount of radioactivity at this time was far too high to see

Received Jan. 1, 1996; revision accepted Jul. 1, 1996.
For correspondence or reprints contact: N. Colas-Linhart, PhD, Faculté de Médecine Xavier Bichat, Laboratoire de Biophysique, BP 416, 75870 Paris, Cedex 18, France.

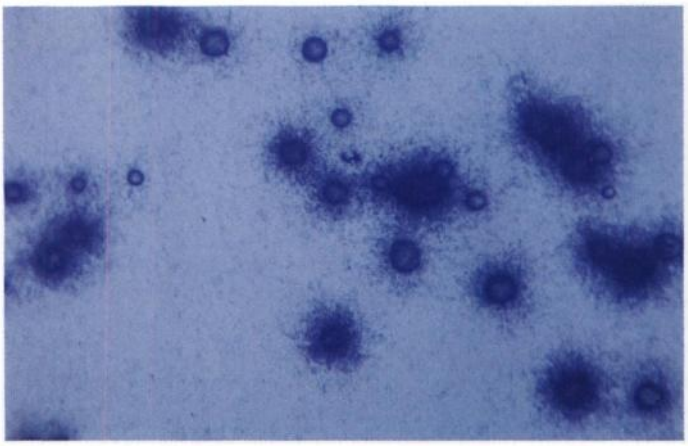

FIGURE 1. Results of MAR performed immediately after microsphere labeling. Differences in individual microsphere radioactivity uptake and size can be seen: microspheres of the same diameter generate different numbers of tracks (magnification ×100) (→).

individual tracks generated by labeled microsphere. Consequently, to avoid overexposure, radioactivity was allowed to decay for 92 hr, at which time slides were coated with the emulsion. After MAR, the number of visible tracks emanating from each microsphere was counted by two observers under an optical microscope. They measured the diameters of the labeled particles and counted the total number of microspheres per slide.

A visualization yield (Y) was calculated to quantify the radioactivity taken up by the microsphere. Briefly, from these counts, a mean number of tracks ($\bar{n}$)/microsphere was determined which

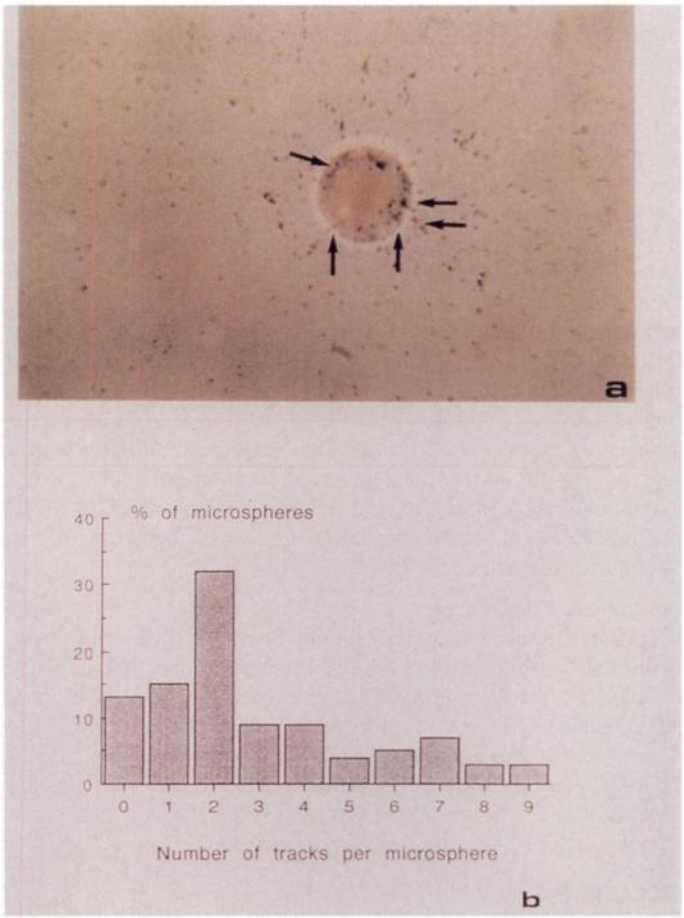

FIGURE 2. Tracks distribution on labeled microspheres. (A) MAR after 92 hr of decay. A microsphere presents five tracks (→) (magnification ×400). (B) Histogram showing the distribution of number of tracks/microsphere after 92 hr of decay.

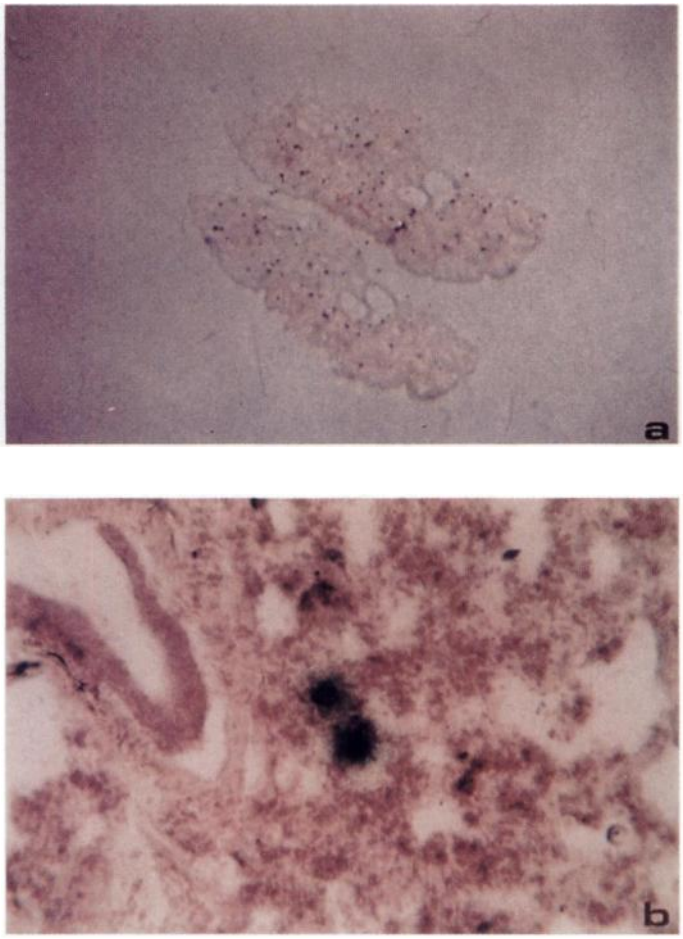

FIGURE 3. Pulmonary distribution of ^{99m}Tc-labeled microspheres. (A) Labeled particles are easily visualized as black spots (magnification 30×). (B) The distribution is very heterogeneous at the tissular level (magnification 100×).

corresponded to a given number of high energy electrons. Each track represented the path of one electron, and 11% of the disintegrations resulted in high energy internal conversion electrons (>100 keV). On the other hand, the radioactivity deposited on each slide, determined by gamma counting, allowed the theoretical mean number of emitted tracks/microsphere ($\bar{t}$) to be calculated as $A.r/N$, where A is the total number of atoms disintegrated during the exposition time (24 hr) on a slide, r is the percentage of high energy electrons emitted/disintegration, and N is the number of particles on the autoradiographed slide. Thus, the visualization yield: $Y(\%) = \bar{n}/\bar{t}.100$.

Animal Studies

These studies were performed in 32 male Wistar rats weighing 320 ± 60 g that were randomly separated into three groups.

A group of 24 animals was injected intravenously with 2.10^5 ^{99m}Tc-labeled microspheres corresponding to an activity of 10 MBq. Three animals were then killed by exsanguination eight different times from 0.25–72 hr after injection. The intact lungs of each animal were removed and their radioactivity content counted. The pulmonary biological half-life of the labeled particles was determined as was their effective half-life.

Another group of five animals was injected with 2.10^5 ^{99m}Tc-labeled particles, corresponding to an activity of 30.5 MBq, and exsanguinated 15 min after injection. The deflated lungs were removed and immediately frozen in liquid nitrogen, and 12 μm-thick serial lung sections were cut on a cryostat. MAR was applied to study the pulmonary microdistribution of the ^{99m}Tc-

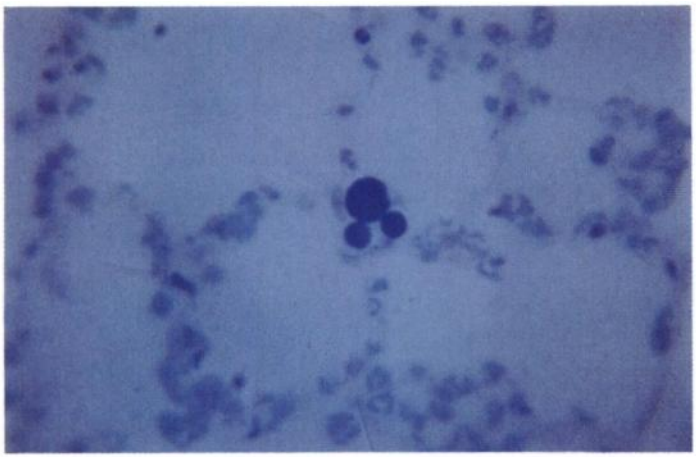

FIGURE 4. Three microspheres trapped in the same capillary (magnification 400×).

labeled microspheres. A 25 μm thick nuclear emulsion was poured onto the lung slices and on control blank slides free of radioactivity to evaluate the nonspecific background level. The distances between labeled microspheres in sections of deflated lungs were measured at high magnification because the nuclear emulsion cannot be used with "frozen specimen-embedding resin" OCT. The length and width of deflated lung sections were also measured.

The lungs of three other control animals were excised intact and were slowly inflated by pouring a mixture of OCT: phosphate buffer into the trachea (*13*). These "inflated" lungs were sectioned, and their lengths and widths were measured. The deflation coefficient (the ratio between deflated and inflated lung areas) was then established and used to correct the distances measured between particles.

Dosimetric Evaluation

From the histological studies (*14*), a schematic anatomical model was established to estimate the doses delivered to the cells in closest contact with the microsphere, i.e., endothelial and type II (PII) epithelial cells. In this study, we considered only electron emissions. The mathematical model applied has previously been described and validated (*15*). Briefly, to calculate the electron ranges and the energy delivered along their path, analytical functions proposed by Prestwich et al. (*16*) and Prestwich et al. (*17*) were used to fit the data published by Berger (*18*). The dosimetric modelization is based on three assumptions: (a) the distribution of radioactivity on the microsphere surface is uniform; (b) only the cells closest to the microsphere are considered and; (c) the mean dose is delivered to the center of the cell considered to be the cell nucleus.

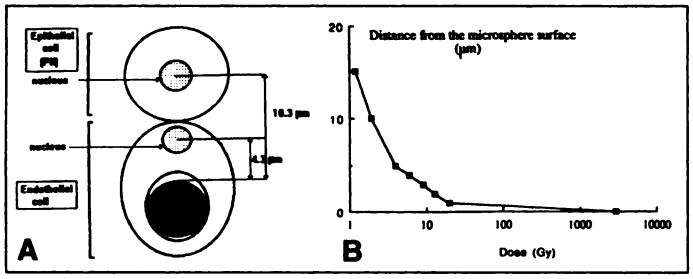

FIGURE 5. Dosimetric studies. (A) A simplified anatomical drawing of an obstructed capillary. The distances between the endothelial and epithelial cells nucleus and the microsphere surface were, respectively, 4.3 and 10.3 μm. (B) Variation of the mean dose delivered as a function of distance from the microsphere surface.

RESULTS

Labeling and Quality Controls

The diameters of the wet particles (n = 280) in suspension ranged from 5–32.5 μm (m ± s.d.: 16 ± 5 μm). No difference in the diameters of unlabeled and labeled microspheres was noted.

On MAR performed immediately after labeling, 100% of the microspheres were labeled (Fig. 1). On these slides, differences in individual radioactivity uptake were observed, with some particles being blacker than others, but this heterogeneity could not be quantified.

After 92 hr of decay time, the number of tracks surrounding individual microspheres could be counted and their distribution assessed (Fig. 2): 87% of the examined microspheres (n = 1830, five experiments) presented 1–9 tracks, and the remaining 13% had none. No correlation was found between the microsphere diameter and the number of tracks (Student's t-test).

A mean of 2.6 tracks/microsphere was observed. The interobserver variation was less than 1%. The visualization yield was Y = 33% ± 3% (m ± s.d. for five experiments). From this visualization yield and under our experimental conditions, the mean initial activity of ^{99m}Tc was 94 Bq/microsphere. Assuming that a linear relationship exists between the number of tracks and the number of ^{99m}Tc atoms taken up by a particular microsphere, the activity per particle ranged from <36 (36 Bq = one track) to 325 Bq (nine tracks).

Animal Studies

Kinetic Studies. Five minutes after injection, more than 90% of the ^{99m}Tc-labeled microspheres were trapped in the lungs. The biological half-life of the labeled particles was 16 hr in rat lungs and was similar to that in mice (*19*). Therefore, the effective half-life of ^{99m}Tc-labeled particles in the lungs was 4.4 hr.

Pulmonary Distribution. Labeled microspheres appeared as black spots and easily identified on MAR preparations at both low and high magnification (Fig. 3). The distribution of labeled particles seems to be uniform at the macroscopic pulmonary level (Fig. 3A). In contrast, at the tissular microscopic level, the distribution was very heterogeneous (Fig. 3B). The deflation coefficient was to 1.43. The distances between labeled microspheres in the lungs corrected with the deflation coefficient varied considerably, ranging from 57–4400 μm. Since the total number of capillaries has been estimated to be $47.10^6/cm^3$ (*20*), one capillary of 2000 was obstructed. Although 90% of microspheres on the examined slices were trapped individually within a given capillary, in some cases, several microspheres were found together within the same capillary (Fig. 4). The background level, observed on control slides corresponding to isolated grains, was very low.

Dosimetric Evaluation

The schematic anatomical model devised to determine the doses and the curve plotting the radiation dose delivered by ^{99m}Tc electrons as a function of the distance from the microsphere surface are shown in Figure 5. When calculated using the mean microsphere diameter (16 μm) the delivered doses ranged from 0.8–7 Gy (using the mean activity = 2 Gy) for the PII epithelial cell nuclei and from 2–21 Gy (using the mean activity = 6 Gy) for the endothelial cell nuclei.

DISCUSSION

One aim of this study was to determine the consequences of the heterogeneous distribution of ^{99m}Tc-labeled microspheres in lungs, using the "track" MAR technique, an experimental tool, very well adapted to the detection of ^{99m}Tc (*10–12*).

MAR performed on suspensions of radiolabeled microspheres is extremely easy to read. The labeled particles were clearly seen as black spots, even at low magnification. Although 100% of the microspheres were labeled in the immediate MAR, the microspheres did not appear to be uniformly labeled. However, the heterogeneity of this labeling could not be quantified on immediate preparations because the signal emitted was too strong. Each particle had not adsorbed the same amount of radioactivity since the number of tracks varied from 0–9. Indeed χ^2 analysis confirmed that this heterogeneity did not conform to Poisson's law of distribution and was therefore related to the labeling rather than to the detection procedure. The mean number of tracks/microsphere was 2.6. The visualization yield (33% ± 3%) calculated for these experiments was high and reproducible. Indeed, it was much higher than for MAR on labeled cells (5%) or tissue sections (1%) (*21*). This difference could be explained by the transparency of the spherical particles that made visible tracks easier to count under the light microscope. This quantification was accurate, as demonstrated by the high counting reproducibility (coefficient of variation ≃10%) and the rather low heterogeneity of activities among microspheres (by a factor ≤10), which was far less than that observed for labeled cells (factor of at least 1000). Using the calculated visualization yield and the number of tracks/microsphere, the range of radioactivity/microsphere could be quantitated.

On pulmonary sections at a macroscopic level, labeled particles were easily visualized as little black spots and seemed uniformly distributed. No difference in distribution was observed as a function of the site within the lung (upper or lower lobe) and also corresponds to the homogeneous appearance of normal human lung scans (*19*). At the microscopic level, the heterogeneous distribution of labeled particles was confirmed as described previously (*9*). The technique also enables this distribution to be visualized and distances between two microspheres to be measured. Interparticle distances varied widely, from 57–4400 μm. Therefore, the distances do not take into account the real tridimentional distribution. Furthermore, we showed that sometimes (10%) more than one microsphere obstructed a capillary, i.e., a distance equal to zero.

These MAR observations clearly demonstrated that several features may vary at the same time: the size of the microsphere, the radioactivity taken up by each microsphere and the distances between microspheres. A mathematical model corresponding to all these data would be difficult to develop, and a symmetrical arrangement of the labeled microspheres in space could not take into account all these variables. Therefore, we used a microsphere of mean diameter (16 μm) labeled with a mean activity (94 Bq) to estimate the radiation doses delivered to the nucleus of endothelial and epithelial cells.

In this study, only the dose delivered to endothelial and epithelial cell nuclei closest to the microspheres was calculated (respectively, 6 and 2 Gy) using the data established by Berger (*18*) in a water medium. These high calculated doses are probably a result of the cell death for these pulmonary cells. However, Tubiana and Bertin (*22*) observed that a 1 Gy dose kills 15%–25% of the pulmonary cells, 2 Gy kill 40%–55% of these cells and beyond 3 Gy, each supplementary Gray kills about 50% of the surviving cells.

The results previously presented by Makrigiorgios et al. (*9*) were obtained from pure computer calculations assuming that all microspheres had the same size, the same amount of radioactivity and the same distance to neighboring particles. Using a cellular dosimetric approach, they demonstrated a high degree of heterogeneity in lung cell irradiation. On the other hand, these authors computed the maximal path of ^{99m}Tc high-energy electrons: 700 μm and a mean distance between two microspheres of 1700 μm. These distances excluded an "overlap" zone, where the probability of cell death was lower, but the probability of carcinogenesis remained (*23*). Our calculations showed that the distance traveled by high energy (142 keV) internal conversion electrons in the intact lung medium was 800 μm. Consequently, the "overlap" zone should be taken into consideration.

Although an extremely inhomogeneous pattern of radionuclide was demonstrated, these findings cannot be directly extrapolated to estimate absorbed doses during lung scanning. In vitro MAR studies performed on microsphere suspensions for human use showed the same size variability and labeling heterogeneity. Because the number of obstructed capillaries in human lungs is lower than in rat lungs, the distances between microspheres should be larger. Nevertheless, the individual doses absorbed by the pulmonary cells closest to the microspheres should be extremely important.

CONCLUSION

Lesions at the tissue and cellular level after radiotherapy have been described in many tissues including lung (*24*) but little is known about potential damage after internal irradiation, like human scan. On the other hand, quantification of biological damage using conventional dosimetry techniques have been unsuccessful (*25*). Further biological studies are needed to estimate the lesions of directly or indirectly exposed cells.

ACKNOWLEDGMENTS

We thank Dr. Françoise Roux of the Pneumology department (Beaujon Hospital, Clichy, France) for valuable comments and discussions. We also thank J.C. Barrault (Sorin Biomedica) for supplying the Sferotec-S kits used in the study. This study is part of the MScD thesis by Marjorie Robinson granted by Electricité de France.

REFERENCES

1. Humm JL, Cobb LM. Nonuniformity of tumor dose in radiotherapy. *J Nucl Med* 1990;31:433–436.
2. Howell RW, Rao DV, Sastry KSR. Macroscopic dosimetry for radioimmunotherapy: nonuniform activity distribution in solid tumors. *Med Phys* 1989;16:66–74.
3. Makrigiorgos GM, Ito S, Baranowska-Kortylewicz J, et al. Inhomogeneous deposition of radiopharmaceuticals at the cellular level: experimental evidence and dosimetric implications. *J Nucl Med* 1990;31:1358–1363.
4. Weber DA, Eckerman KF, Thomas Dillman L, Ryman JC. *MIRD radionuclide data and decay schemes*. New York: Society of Nuclear Medicine, 1989.
5. Zolle I, Rhodes BA, Wagner HN Jr. Properties and uses of radioactive albumin microspheres [Abstract]. *J Nucl Med* 1968;9:363.
6. Kowalsky RJ, Perry JR. In: Appleton et Lange, eds. *Radiopharmaceuticals in nuclear medicine practice*. Norwalk, CT; 1987.
7. Gardin I, Colas-Linhart N, Petiet A, Bok B. Dosimetry at the cellular level of Kupffer cells after technetium-99m-sulphur colloid injection. *J Nucl Med* 1992;33:380–384.
8. Loevinger R, Berman M. *A revised schema for calculating the absorbed dose for biologically distributed radionuclides*. New York: Society of Nuclear Medicine; 1976: MIRD pamphlet 1, revised.
9. Makrigiorgos GM, Aldelstein SJ, Kassis AI. Cellular radiation dosimetry and its implications for estimation of radiation risks. *JAMA* 1990;264:592–595.
10. Barbu M, Colas-Linhart N, Bok B. Technetium-99m autoradiography of labeled white cells. *Acta Haemat* 1984;71:13–14.
11. Fourré C, Petiet A, Colas-Linhart N. Prospects in technetium dosimetry at the cellular level: mutual contribution by "track" microautoradiography method (MAR) and secondary ion mass spectrometry (SIMS) microscopy. *Mol Cell Biol* 1996;42:385–393.
12. Hindie E, Colas-Linhart N, Petiet A, Bok B. Microautoradiographic study of technetium-99m colloid uptake by the rat liver. *J Nucl Med* 1988;29:1118–1121.
13. Edelson JD, Shannon JM, Mason RJ. Alkaline phosphatase: a marker of alveolar type II cell differentiation. *Am Rev Respir Dis* 1988;138:1268–1275.
14. Haies DM, Gil J, Weibel ER. Morphometric study of rat lung cells. I. Numerical and dimensional characteristics of parenchymal cell population. *Am Rev Respir Dis* 1981;123:533–541.
15. Faraggi M, Gardin I, De Labriolle-Vaylet C, Moretti JL, Bok BD. The influence of tracer localization on the electron dose rate delivered to the cell nucleus. *J Nucl Med* 1994;35:113–119.
16. Prestwich WV, Chan L, Kwok CS, Wilson B. Dose point kernels for beta-emitting radioisotopes. *Proceedings of the 4th international radiopharmaceutical dosimetry symposium*. Conf-851113 Oak Ridge, TN: 1985:545–561.
17. Prestwich WV, Numes J, Kwok CS. Beta doses point kernels for radionuclides: potential use in radioimmunotherapy. *J Nucl Med* 1989;30:1036–1046.

18. Berger MJ. *Improved point kernels for electron and beta ray dosimetry*. Washington DC: U.S. Department of Commerce, National Bureau of Standards; 1973:73–107.
19. Rhodes BA, Stern HS, Buchanan JA, Zolle I, Wagner HN. Lung scanning with ^{99m}Tc microspheres. *Radiology* 1971;99:613–621.
20. Weibel ER, ed. *Morphometry of the human lung*. New York: Academic Press; 1963:81–82.
21. De Labriolle-Vaylet C, Colas-Linhart N, Petiet A, Bok B. Morphological and functional status of leucocytes labeled with ^{99m}Tc-HMPAO. In: Sinzinger H, Thakur ML, eds. *Radiolabeled cellular blood elements*. New York: Wiley-Liss; 1990:119–129.
22. Tubiana M, Bertin M, eds. *Radiobiology radioprotection*. Paris, France; Presses Universitaires de France; 1989:43–44.
23. Kassis AI, Adelstein SJ. Does nonuniformity of dose have implications for radiation protection? *J Nucl Med* 1992;33:384–387.
24. Rodemann HP, Bamberg M. Cellular basis of radiation-induced fibrosis. *Radiother Oncol* 1995;35:83–90.
25. Watt DE, Khan S. *Cross-sections for the biological effectiveness of electrons in mammalians cells*. Lund, Sweden: Third International Symposium on Biophysical Aspects of Auger Processes; 1995:L13.

Simplifying the Dosimetry of Carbon-11-Labeled Radiopharmaceuticals

Mark C. Wrobel, James E. Carey, Phillip S. Sherman and Micheal R. Kilbourn
Division of Nuclear Medicine, Department of Internal Medicine, University of Michigan, Ann Arbor, Michigan

A two time-point sacrifice method is proposed as an alternative to conventional multiple time-point sacrifice methods to determine the organ cumulated activity of ^{11}C-labeled radiopharmaceuticals. **Methods:** Rat biodistribution data for 10 ^{11}C-labeled radiopharmaceuticals were analyzed to determine organ cumulated activity. Data were obtained at four sacrifice intervals 2–5 min, 10–15 min, 30–45 min and 1–1.5 hr postinjection. The organ absorbed dose per unit administered radioactivity (mGy/MBq) was calculated using all four data points and combinations of limited data. The objective was to determine if a limited sampling technique would provide sufficient accuracy in estimating absorbed dose. **Results:** Residence times calculated using two time-points acquired during the first half-life of ^{11}C were either equivalent or positively biased compared to using all sacrifice times. Overall, 87% of the residence times assessed were conservative compared to the multipoint method. For bladder organs, a consistent negative bias was observed with the reduced sacrifice method. **Conclusion:** Analysis of animal biodistributions using a reduced sacrifice protocol provides results in good agreement with and generally conservative to results using all sacrifice intervals. Correction factors are required for the urinary bladder and gallbladder when using the simplified technique due to bias. The bladder was often the limiting organ in determining human administered activity.

Key Words: dosimetry; PET; carbon-11

J Nucl Med 1997; 38:654–660

Human absorbed dose from ^{11}C-labeled radiopharmaceuticals is initially estimated using animal tissue and organ biodistributions (*1*), typically in the rat. For a new ^{11}C-labeled radiotracer, this determination will usually include measuring organ activities at four or five time-points during the first three or four physical half-lives of ^{11}C, using four to six animals per time-point. Organ time-radioactivity profiles are obtained from the measured organ radioactivity and cumulated activity, residence time and organ absorbed dose per unit administered radioactivity are calculated (*2,3*).

Determination of animal radioactivity biodistributions for ^{11}C-labeled radiotracers is not trivial. Difficulties include the short (20 min) physical half-life requiring a rapid sacrifice protocol and the use of a significant number of animals to provide high precision and accuracy in the determination. These issues have been recognized by Gatley (*4*), who recommended eliminating animal measurements and basing dose estimates on human cardiac output models. In addition, Schaumann et al. (*5*) recommended limiting the sacrifice data for long lived ^{14}C-labeled agents. In contrast, we evaluated the use of a simplified technique which uses only two sacrifice intervals to assess residence time. Using animal biodistribution data for 10 ^{11}C-labeled radiopharmaceuticals, we compared dosimetry estimates with the simplified technique and showed that such an alteration yields acceptable estimates of the expected human dosimetry.

The accurate assessment of urinary bladder-wall dose and gallbladder-wall dose are often overlooked when evaluating new short-lived radiotracers. This is partly due to the difficulty of measuring the residence time for these organs as well as the perception that because of delayed filling and the short physical half-life of ^{11}C, they will be of lesser dosimetric importance than organs that receive first-pass depositions from the blood pool. The urinary bladder contents and estimated gallbladder contents residence times in the rat for 10 ^{11}C radiotracers were estimated using measured organ activities and a set of conservative assumptions based on ICRP-53 recommendations (*6*). Results indicate that the bladder organs can be critical in determining the limiting dose of new ^{11}C-labeled radiotracers for human patients.

THEORY

Given a single bolus injection of radioactivity, A_o, into the blood pool, the radioactivity in organ or tissue S can be estimated using the compartmental model:

$$\frac{A_s(t)}{A_o} = F_s \sum_{j=n+1}^{n+m} a_j \sum_{i=1}^{n} \left\{ a_i \frac{\lambda_j}{\lambda_j - \lambda_i} [\exp - (\lambda_i + \lambda_p)t - \exp - (\lambda_j + \lambda_p)t] \right\}, \quad \text{Eq. 1}$$

where F_s is the fractional distribution to organ or tissue S; a_i is the fraction of F_s eliminated with biological removal constant λ_i; a_j is the fraction of F_s taken up with biological uptake constant λ_j; n is the number of elimination components; m is the number of uptake components; and λ_p is the physical decay constant (*6*).

For absorbed dose calculations in nuclear medicine, and, in particular, for short half-life tracers ($T_{1/2} \leq 20$ min), several simplifying assumptions to the above model may be applied. First, uptake is either based on a single component, or instantaneous uptake is assumed (*6*). Further, the effective removal of radioactivity from an organ is described by a single component, and short half-life radiotracers can be taken to be equal to the physical decay constant (*6*). With single uptake and excretion components, the above model becomes:

$$\frac{A_s(t)}{A_o} = F_s \times \frac{\lambda_j}{(\lambda_j - \lambda_i)} [\exp - (\lambda_i + \lambda_p)t - \exp - (\lambda_j + \lambda_p)t]. \quad \text{Eq. 2}$$

Received Apr. 8, 1996; revision accepted Jun. 28, 1996.
For correspondence or reprints contact: James E. Carey, MS, University of Michigan Medical Center, Division of Nuclear Medicine, B1G505, University Hospitals, Ann Arbor, MI 48109-0028.